

# PCCP

Accepted Manuscript



This is an *Accepted Manuscript*, which has been through the Royal Society of Chemistry peer review process and has been accepted for publication.

*Accepted Manuscripts* are published online shortly after acceptance, before technical editing, formatting and proof reading. Using this free service, authors can make their results available to the community, in citable form, before we publish the edited article. We will replace this *Accepted Manuscript* with the edited and formatted *Advance Article* as soon as it is available.

You can find more information about *Accepted Manuscripts* in the [Information for Authors](#).

Please note that technical editing may introduce minor changes to the text and/or graphics, which may alter content. The journal's standard [Terms & Conditions](#) and the [Ethical guidelines](#) still apply. In no event shall the Royal Society of Chemistry be held responsible for any errors or omissions in this *Accepted Manuscript* or any consequences arising from the use of any information it contains.

# Pits Assisted Oxygen Chemisorption on GaN Surfaces

Monu Mishra<sup>†§</sup>, Shibin Krishna TC<sup>†§</sup>, Neha Aggarwal<sup>†§</sup>, Mandeep Kaur<sup>§</sup>, Sandeep Singh<sup>#</sup> and Govind Gupta<sup>†§\*</sup>

<sup>†</sup> Surface Physics and Nanostructure Heteroepitaxy, Physics of Energy Harvesting Division, CSIR-National Physical Laboratory, Dr. K.S. Krishnan Marg, New Delhi-110012, India.

<sup>§</sup> Quantum Phenomena and Applications, CSIR-National Physical Laboratory, Dr. K.S. Krishnan Road, New Delhi-110012, India.

<sup>#</sup> Sophisticated and Analytical Instrumentation, CSIR-National Physical Laboratory, Dr. K.S. Krishnan Road, New Delhi-110012, India.

<sup>§</sup> Academy of Scientific and Innovative Research (AcSIR), CSIR-NPL Campus, Dr. K.S. Krishnan Road, New Delhi-110012, India.

\*Corresponding Author: [govind@nplindia.org](mailto:govind@nplindia.org)

## Abstract

A comprehensive analysis of oxygen chemisorption on epitaxial gallium nitride (GaN) films grown at different substrate temperatures via RF-Molecular Beam Epitaxy is carried out. Photoemission (XPS & UPS) measurements were performed to investigate the nature of surface oxide and corresponding changes in the electronic structure. It was observed that the growth of GaN films at lower temperature lead to lower amount of surface oxide, however vice versa was perceived for higher temperature growth. The XPS core level (CL) and valence band maximum (VBM) position shifted towards higher binding energy (BE) with oxide coverage and revealed a downward band bending. XPS valence band spectra were de-convoluted to understand the nature of hybridization states. UPS analysis divulged higher values of electronic affinity and ionization energy for GaN films grown at higher substrate temperature. The surface morphology and pit structure were probed via microscopic measurements (FESEM & AFM). FESEM and AFM analysis revealed that surface was covered with hexagonal pits which played a significant role in oxygen chemisorption. The favourable energetics of the pits offered an ideal site for oxygen adsorption. Pit density and pit depth were observed to be important parameters governing the surface oxide coverage. The contribution of surface oxide was increased with increase in average pit density as well as pit depth.

**Keywords:** GaN, Chemisorption, Photoemission, Microscopy, Oxide.

## Introduction:

Understanding of surface properties is of key importance for the design, characterization and development of III-Nitrides based noble device structures. Surface properties play a crucial role in governing the performance of these devices. They assist various technological issues like surface states<sup>1,2</sup>, Fermi level pinning (or unpinning)<sup>1,3</sup>, band bending<sup>2-4</sup>, quality of metal contact<sup>5,6</sup>, leakage current<sup>7,8</sup>, current collapse<sup>7,9</sup>, etc. Theoretical and experimental analysis of oxygen chemisorption on GaN surfaces were initiated by Elsner<sup>10</sup> and Bermudez et al.<sup>11</sup> They reported that the chemisorption of oxygen lead to increase in work function and electron affinity of the films. In order to fabricate high quality metal/semiconductor contact, it was observed that Aluminium deposited on GaN surface reacts with surface oxide and forms Al<sub>2</sub>O<sub>3</sub>.<sup>12</sup> The quality of metallization and Schottky barrier formation are significantly altered by the surface oxide.<sup>13</sup> Shalish et al.<sup>14</sup> analysed the correlation

between surface oxide (gallium oxide) with yellow luminescence and reported that the presence of oxygen on the surface decorates grain boundaries and produces defect related yellow luminescence. Previous reports have proposed that oxygen can produce native gate oxide<sup>15</sup> and the oxygen related traps can increase the gate leakage.<sup>16</sup> In a recent study, it was reported that the oxide particles (Ga<sub>2</sub>O<sub>3</sub>) lead to the OFF-state degradation of AlGaIn/GaN high electron mobility transistors.<sup>17</sup> These studies indicates the necessity to have a better understanding of oxygen chemisorption on GaN surfaces.

It is well understood that the surface morphology of the grown GaN films can vary due to growth kinetics<sup>18,19</sup>. It has been observed that GaN surfaces exhibit pits on the surface<sup>20</sup>. These pits possess different energetics<sup>21</sup> than flat surface and may act as a favourable site for oxygen adsorption. However, even being so important, this area is relatively unexplored and lacks

scientific attention. Hence, it would be interesting to investigate and analyse the effect of surface pits on oxygen chemisorption and electronic structure of the grown films. To the best of our knowledge, it would be the first study that compares and correlates the structures of the pits with oxygen chemisorption on the surface. In the present study, a systematic photoemission (XPS & UPS) analysis has been carried out to analyse the surface oxide coverage and its effect on the electronic properties. The nature of surface oxide and the valence band hybridization states were also analysed. We have correlated the surface oxygen chemisorption with surface morphology and pit structures.

### Experimental:

The growth of undoped crystalline GaN films (1  $\mu\text{m}$  thick) was carried out on commercially purchased MOCVD grown GaN template (GaN/c-sapphire) via RIBER RF-Plasma Assisted Molecular Beam Epitaxy (PAMBE). The films were grown at three different substrate temperatures namely 720°C (sample 1), 730°C (sample 2) and 740°C (sample 3) under identical Ga/N flux ratio and RF power of 500W. The samples are abbreviated as S1, S2 and S3 respectively, in the present report. Photoemission (XPS & UPS) experiments were performed in Ultra-high Vacuum (UHV) based system (OMICRON Multiprobe Surface Analysis System) operating at a base pressure of  $5 \times 10^{-11}$  Torr. Samples were ultrasonicated in acetone for 10 min to remove the physisorbed contaminations prior to introduction in UHV chamber. No chemical etching was employed to clean the samples as they may etch the surface and alter the coverage of chemisorbed surface oxygen. Samples were mounted on molybdenum plates using conductive tape with silver contacts on the edges to avoid charging; however the system was also equipped with a charge neutralization facility to eliminate the additional build-up charge during the measurement. The XPS measurements were carried out using both  $\text{MgK}_{\alpha}$  (1253.6 eV) and monochromatized  $\text{AlK}_{\alpha}$  (1486.7 eV) radiation sources. Monochromatized  $\text{AlK}_{\alpha}$  radiation was employed to determine the exact position of C (1s) core level due to the masking occurred by Ga (LMM) Auger lines via  $\text{MgK}_{\alpha}$  radiation. Ultraviolet photoelectron spectra (UPS) were obtained using in-situ discharge lamp (OMICRON HIS 13) with He (I) (21.2 eV) radiation. The calibration of work

function of the system and the binding energy in photoemission spectra was carried out referring to Au 4f<sub>7/2</sub> emission line and Au Fermi level. The core level (CL) curve fitting was done using Shirley background and Voigt (mixed Lorentzian-Gaussian) line shape calibrated against C (1s) binding energy of 284.8 eV. The VB maximum (VBM) position was determined by extrapolating a linear fit to the leading edge of the valence band photoemission to the baseline.<sup>22,23</sup> Surface morphology and pit structure were probed by Atomic Force Microscopy (AFM, Multimode-V Veeco) and Field-emission Scanning Electron Microscopy (FESEM, ZEISS AURIGA).

### Results and discussion:

To investigate the surface oxide coverage and the interaction of chemisorbed oxygen with the surface of the films, systematic XPS measurements were performed. Figure 1 shows the de-convoluted XPS Ga (3d) CL spectra of sample 1, 2 and 3 observed at binding energy (BE) position of 19.5 eV, 19.7 eV and 20.0 eV, respectively. The peaks were de-convoluted into three major components attributed to Ga-Ga ( $18.5 \pm 0.1$  eV), Ga-N ( $19.7 \pm 0.1$  eV) and Ga-O ( $20.7 \pm 0.1$  eV) bonding.<sup>22-24</sup> Table 1 represents the FWHM and percentage contribution of the observed components in Ga (3d) CL spectra. The shift of the Ga (3d) CL towards higher BE (0.2 eV for S2 and 0.5 eV for S3) and increment in the FWHM revealed higher amount of surface oxide. Further, the shifts in the CL also indicate towards strong downward band bending (from S1 to S3). The degree of band bending in the grown GaN films increased from S1 to S3. The observed downward band bending is an indication of large concentration of surface states (surface oxides, contaminants etc.) in the grown films. These states can pin the Fermi Level and produce significant effect on the VB offset in the heterostructures. We observed that the contribution of surface oxide increased from S1 to S3. However, the contribution of metallic gallium decreased significantly (absent in S3). The de-convoluted XPS O (1s) CL spectra are shown in Figure 2. The identified components were attributed to chemisorbed oxygen (in the form of  $\text{Ga}_x\text{O}_y$  and  $\text{Ga}_2\text{O}_3$ ) and hydroxyl species (due to adsorption of water on the surface)<sup>22</sup> located at BE of  $530.2 \pm 0.1$  eV,  $531.4 \pm 0.1$  eV and  $532.8 \pm 0.1$  eV, respectively. Several experimental<sup>25,26</sup> and theoretical<sup>27,28</sup>

investigations of water adsorption on GaN surfaces have performed in recent years. The studies indicated towards the aqueous stability<sup>26</sup> of the GaN films with very low coverage of adsorbed water molecules (OH species).<sup>27</sup> The GaN films were observed to be more reactive to molecular oxygen than molecular water in air ambient conditions.<sup>25-28</sup> First principle calculations revealed that the coverage of hydroxyl species could be up to 0.75 monolayers.<sup>28</sup> The de-convoluted O (1s) CL spectra also shows a decrease in the hydroxyl species in the present study. No significant shifts in the CL spectra were observed but the FWHM followed an interesting pattern. FWHM of the peaks varied from 2.78 to 2.13 (see table 1). The lower FWHM of S2 and S3 were attributed to the minimal contribution from the Ga<sub>x</sub>O<sub>y</sub> species as shown in Figure 2 (b & c). The contribution of chemisorbed oxygen increased from S1 to S3; however S2 divulged absence of Ga<sub>x</sub>O<sub>y</sub> bonding (see table 1). The chemisorbed oxygen was perceived to be of Ga<sub>2</sub>O<sub>3</sub> in nature due to its lower Gibbs free energy. The CL analysis confirmed that the amount of chemisorbed oxygen was increased from S1 to S3 and the nature of chemisorbed oxygen is dominated by Ga<sub>2</sub>O<sub>3</sub> bonding.

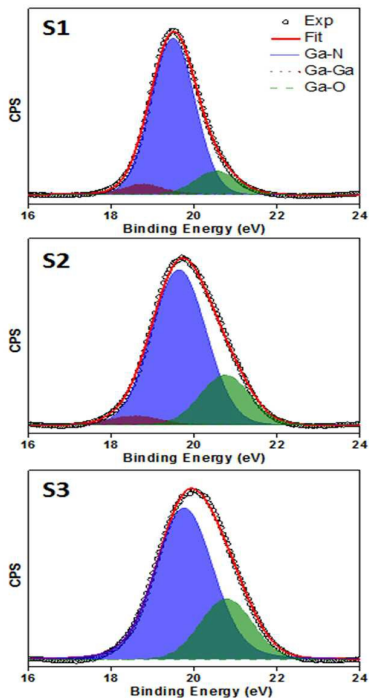


**Figure 1:** (Color online) De-convoluted Ga (3d) XPS spectra of sample 1(S1), 2 (S2) and 3 (S3) displaying various components. Open circles showing experimental data while solid lines are fitted curves.

**Table 1:** Peak positions, FWHM and the percentage contribution of different components in the de-convoluted Ga (3d) and O (1s) core level of the grown GaN films.

		Sample 1	Sample 2	Sample 3
Ga 3d	Position (eV)	19.5	19.7	20.0
	FWHM	1.84	2.42	2.58
	Metallic Ga (%)	8	4	-
	GaN (%)	81	77	74
	Ga-O (%)	11	19	26
O 1s	Position (eV)	531.5	531.4	531.4
	FWHM	2.78	2.13	2.40
	Ga <sub>x</sub> O <sub>y</sub> (%)	15	-	4
	Ga <sub>2</sub> O <sub>3</sub> (%)	60	77	79
	Hydroxyl (%)	25	23	17

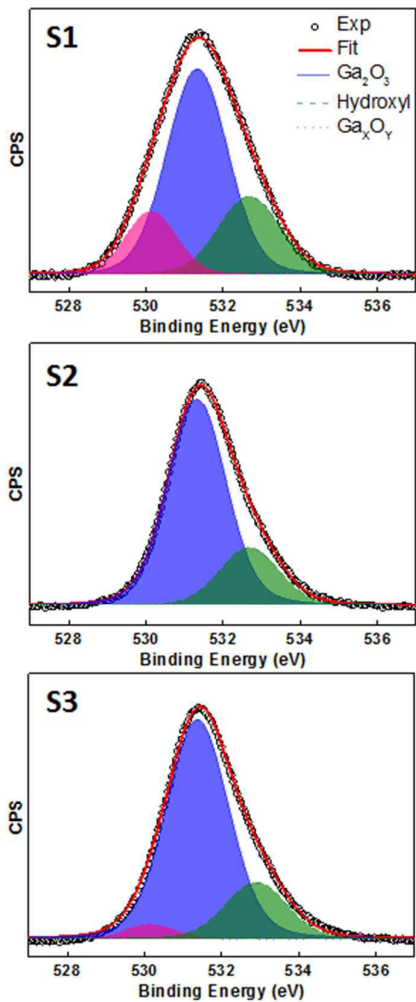


**Figure 2:** (Color online) De-convoluted O (1s) XPS spectra of S1, S2 and S3 displaying various components.



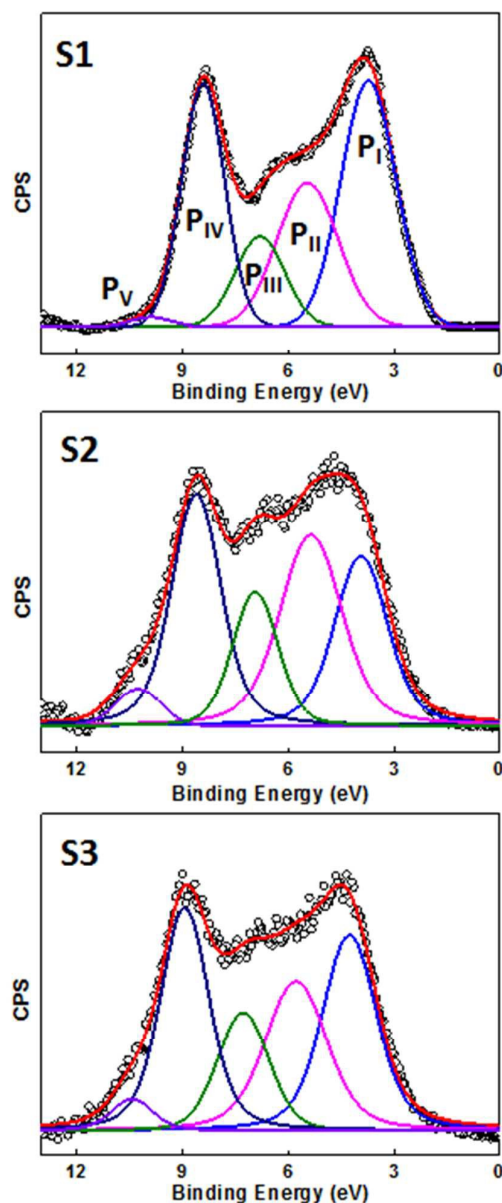


**Figure 3:** (Color online) De-convoluted XPS valence band spectra of the GaN films using monochromatized AlK $\alpha$  (1486.7 eV) excitation representing the hybridization states.

For the analysis of electronic structure and the valence band hybridization states, samples were characterized via monochromatized AlK $\alpha$  excitation as shown in Figure 3. The VBM positions were calculated to be  $2.0 \pm 0.1$  eV,  $2.2 \pm 0.1$  eV and  $2.6 \pm 0.1$  eV below the Fermi Level (FL) for S1, S2 and S3 respectively. The high value of VBM for S3 was attributed to the presence of higher surface oxide<sup>22,23</sup> as evident from the de-convoluted Ga (3d) CL spectra. The energy separation between Ga (3d) CL and VBM [i.e.  $E_{\text{CL-VBM}}$ ] which is a material property, was

obtained to be nearly identical (17.5 eV) for all the samples and lies within the reported values of 17.1-18.4 eV.<sup>22</sup> The obtained valence band spectrum was in agreement with the theoretical<sup>29</sup> as well as experimental<sup>30</sup> studies. The de-convolution of the VB spectra was performed to understand the nature of hybridization states after reviewing the available literature reports.<sup>29-33</sup> The de-convoluted VB spectra for the samples revealed five identified peaks labelled as P<sub>I</sub>, P<sub>II</sub>, P<sub>III</sub>, P<sub>IV</sub> and P<sub>V</sub>. The positions and the corresponding hybridization states of the mentioned peaks are tabulated in Table 2. These peaks denote to the N2p-Ga4p<sup>31-33</sup>, N2p-Ga4s\*<sup>24</sup>, mixed orbitals<sup>31,32</sup> (or surface adsorbates) and N2p-Ga4s<sup>31-33</sup> hybridization states along with a small satellite peak.<sup>24,33</sup> The N2p-Ga4s\* corresponds to slightly higher energy, but due to the non-zero density of states, was ascribed to this energy. The better explanation for locating the peak at above mentioned position can be found in earlier reports.<sup>24,33</sup> The de-convolution divulged that the valence band hybridization states correspond to the interactions of Ga 4s and Ga 4p orbitals with N 2p orbital. The intensity of hybridization states was observed to vary with oxide coverage (see Fig. 3). The reason behind this variation is still not known and needed to be explored more. The position of the peaks was observed to be shifted towards higher BE (S1 to S3). Previous studies<sup>34,35</sup> have reported that the pinning or defect states related to either gallium dangling bonds or nitrogen vacancies are located at  $\sim 0.5$ - $0.7$  eV below the conduction band edge. Since the VBM position for S3 is in the close vicinity of the value ( $\sim 0.8$  eV below the conduction band edge), it was expected that the sample possess gallium dangling bonds. The dangling bonds can offer a favourite site for oxygen adsorption (due to the strong difference in the electronegativity) and higher amount of surface oxide. The observed results and above explained mechanism justifies the higher amount of oxide in sample S3 in an appropriate manner.

**Table 2:** Energy separation and Peak positions for the hybridized levels as observed from the convoluted valence band spectra from the GaN samples.

	Peak Positions (eV)			
	Sample 1	Sample 2	Sample 3	Hybridization
$E_{\text{CL-VBM}}$	17.5	17.5	17.4	-
Peak 1 (P <sub>I</sub> )	3.73	3.92	4.28	N 2p-Ga 4p (p-like)
Peak 2 (P <sub>II</sub> )	5.45	5.42	5.78	N 2p-Ga 4s*
Peak 3 (P <sub>III</sub> )	6.82	6.96	7.30	Mixed (adsorbate)
Peak 4 (P <sub>IV</sub> )	8.41	8.60	8.91	N 2p-Ga 4s (s-like)
Peak 5 (P <sub>V</sub> )	9.92	10.27	10.46	Satellite

To analyse the energy band structure (estimated by the position of surface FL and is one of the most important parameter in governing the performance of devices) and electronic properties, UPS measurements of the samples were performed. Figure 4 shows the observed UPS VB spectra [Fig. 4(a)] and band structure [Fig. 4(b)] of the samples. The intensity of the peak located at ~15.0 eV was observed to be completely suppressed from S1 to S3, however that of the peak at ~13.5 eV was minimized slightly. The major difference between the samples is the presence of metallic gallium and the amount of surface oxide. Hence, it was expected that the peak (at ~15.0 eV) belongs to metallic gallium (or Ga-N bonds) and therefore was highly suppressed in S3 (due to the absence of metallic gallium). The UPS VBM values were calculated to be  $3.4 \pm 0.1$  eV,  $3.8 \pm 0.1$  eV and  $3.95 \pm 0.1$  eV for sample S1, S2 and S3 respectively. The FL of the samples was observed to be above the conduction band minimum (CBM) and followed the similar trend like XPS.

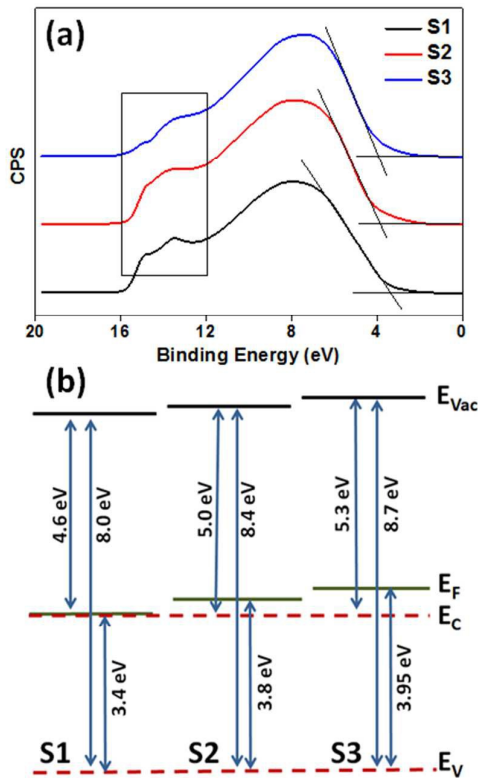


**Figure 4:** (Color online) a) UPS valence band spectra acquired using He (I) (21.2 eV) radiation, and b) band-structure diagram of the GaN films

The electron affinity ( $\chi$ ) was determined using UPS spectra via following equation:

$$\chi = h\nu - W - E_g. \quad [1]$$

where,  $h\nu$  is the energy of the incident photons,  $W$  is the spectral width and  $E_g$  is the band gap (3.4 eV) of the material.<sup>22</sup> The photo threshold energy or the ionization energy of the electrons is the energy difference between the UPS photon energy and the spectrum width or the sum of the electron affinity and band gap. The calculated values of the electron affinity (and ionization energy) and the schematic band structure diagram of the samples are shown in Fig. 4(b). The higher values of electron affinity and ionization energy for sample S2 and S3 corresponds to the presence of surface oxides.<sup>36</sup>

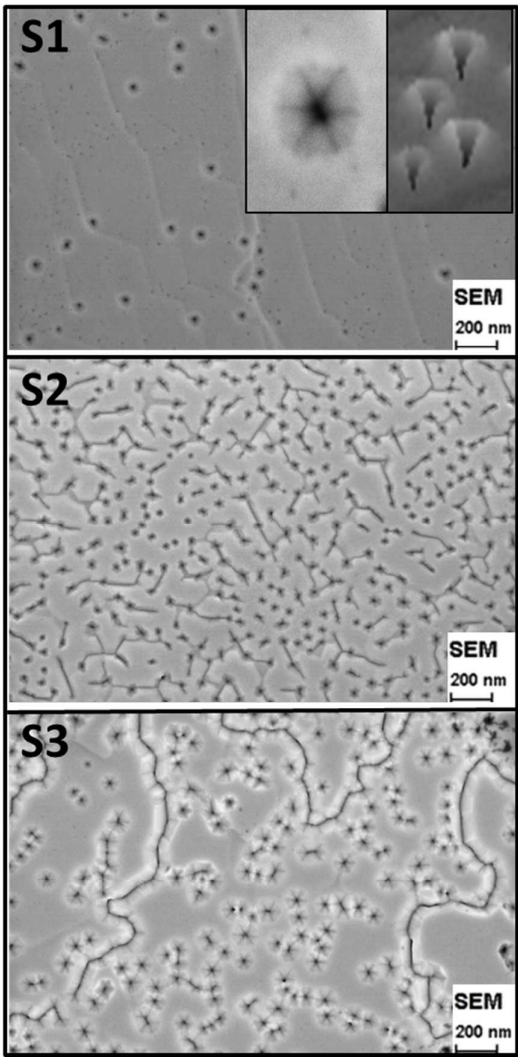


**Figure 5:** (Color online) Field Emission SEM images of the GaN films showing surface morphology and the hexagonal pits.

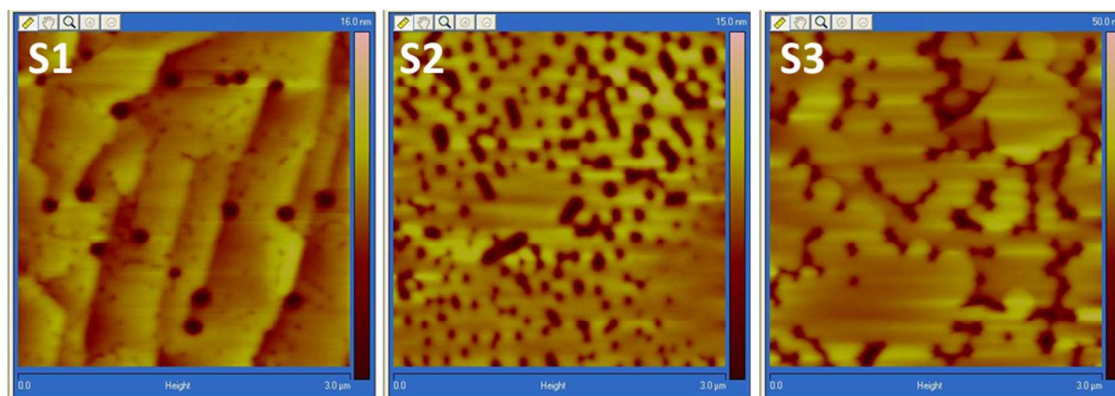


**Figure 6:** (Color online) AFM images of the samples of the GaN films displaying step flow growth and flat terraces along with surface pits.

The photoemission measurements confirmed that S3 possess the highest amount of surface oxide and absence of metallic gallium. Hence, to correlate the surface oxide with the morphology of the grown films, microscopic (FESEM and AFM) measurements were performed. The root mean square (rms) roughness, average pit depth and pit density of the samples are represented in table 3. The plan-view FESEM images of the samples are shown in Figure 5. Surface of the films were observed to be covered with small hexagonal pits which have a V-shape in cross section (as shown in the inset of Fig. 5).<sup>37-39</sup> The side walls of the individual pit is defined by six  $(10\bar{1}1)$  facets, but they start adjoining when the density of pits are large [Fig 5(b) and 5(c)]. The side wall then appears form  $(10\bar{1}3)$  or  $(10\bar{1}4)$  plane, rather than the  $(10\bar{1}1)$  facet.<sup>38</sup> The adjoining of the facets was observed in S2 and S3 due to the high density of surface pits. It is well understood that the number density, size and depth of these pits are dependent on growth conditions. We have grown the samples at different temperatures, so it was expected that samples may exhibit different morphologies.<sup>38</sup> For the accurate explanation of oxygen adsorption, it is essential to understand the energetics of these pits. Kim et al.<sup>39</sup> reported that the film become more tensile from outer area to the centre of the pit via exhibiting a biaxial stress of 0.13 GPa between them. Previous studies reported that these pits possess higher energy<sup>37</sup> and the concentration of electron inside the pit is much higher than outside the pit.<sup>40</sup> The major cause for the formation of these surface pits are attributed to the defect structures (dislocations)<sup>39,40</sup> but in the present scenario the films are grown on MOCVD-GaN template. Hence it was expected that the defect structure

should remain constant throughout the grown samples.. A STEM study by Hawkridge et al.<sup>41</sup> suggested that the Oxygen content increases replacing Nitrogen inside a dislocation and while the Gallium content remains intact. They also proposed that Oxygen can accumulate at surface pits and completely substitute the nitrogen on facets. Since the energy inside the pits is higher and Oxygen coverage can produce sufficient change in the energy, we expect that the Oxygen would have substituted Nitrogen and interacted with the residual Gallium to form oxides of Gallium (Ga-O) inside the pits. The aforementioned explanations support that the pits are an ideal site for the oxygen adsorption on the surface. Butcher et al.<sup>42</sup> reported that the coalescence of dislocations allows higher amount of oxygen on the surface, which is in well agreement with our results. Sample S2 and S3 show coalescence of surface pits and divulge higher amount of surface oxide.

**Table 3:** RMS roughness, average pit depth and density of the GaN samples.

Photoemission and FESEM measurements			
	Pit Density ( $\times 10^8 \text{ cm}^{-2}$ )	Avg. Pit Depth (nm)	Roughness (nm)
<b>Sample 1</b>	0.16	11	1.75
<b>Sample 2</b>	15.7	7	2.02
<b>Sample 3</b>	13.5	16	5.11

revealed that oxide coverage is directly related to the pit density. The contribution of surface oxide (Ga-O) was increased with increase in pit density from S1 to S3 (table 1 and 3). However, it was interesting to see that the contribution was observed to be higher for sample S3 which had a lower pit density. Hence we performed the AFM



measurements of the samples for the better correlation and understanding of the adsorption mechanism. The AFM images of the grown GaN films are shown in Figure 6. Surface of the samples showed step flow growth and areas of flat terraces along with few pits.<sup>43</sup> The rms roughness and average pit depth of the samples are mentioned in table 3. The average pit depth was observed to be highest for S3. Comparing S2 and S3, we observed that the average pit depth and pit density varied from 7 nm to 16 nm and  $15.7 (\times 10^8 \text{ cm}^{-2})$  to  $13.5 (\times 10^8 \text{ cm}^{-2})$ , respectively. There was significant variation ( $\sim 2.3$  times) in average pit depth from S2 and S3. The larger pit depth was an outcome of grouping (coalescence) of pits as evident from AFM as well as FESEM analysis. Thus, we observed that the increase in oxide component for S3 was an outcome of pit depth. The AFM analysis concluded that the pit density is not the only parameter affecting the oxygen chemisorption but it depends on pit depth as well. The rms roughness of the samples was observed to be increased from S1 to S3. The increase in surface roughness was attributed to two major reasons namely (i) adsorption of oxygen and (ii) presence of metallic gallium.<sup>38,42</sup>

The low roughness in S1 and S2 was attributed to the mobility of metallic gallium<sup>43</sup> (see photoemission part). The presence of metallic gallium lead a two dimensional growth and increased adatom mobility. The high mobility of these adatoms favours migration of atoms in order to reduce the surface free energy. The density functional calculation states that delocalized Ga-Ga bonds possess very low barrier to surface migration.<sup>44</sup> Metallic gallium (Ga-Ga species) in S1 and S2 encourages the covering of the pits and hence a smooth and less pitted surface was formed. However in case of S3, there was not metallic gallium species but surface oxide. The oxygen may have less adatom mobility and the surface possess high energy barrier due to different surface kinetics. The migration of adatoms was low and thus formed a rough surface. Thus it can be assumed that surface oxide also plays a significant role in governing the morphology (pits as well as roughness) of the grown films. The pit assisted oxygen chemisorption lead to significant change in electronic structure as well.

In summary, oxygen chemisorption on GaN surfaces was analysed. Surface oxidation lead to shifts in core levels as well as valence band spectra. Hybridization states of the valence band were investigated. It was observed that pits play

a significant role in surface oxidation and are favourable site for oxygen adsorption. The contribution of surface oxide increased with pit density as well as average pit depth. The roughness of the films was also found to be increased with increase in surface oxide.

## Conclusion:

Oxygen chemisorption on GaN films grown at different temperatures was analysed via Photoemission and Microscopic (FESEM and AFM) techniques. Surface oxidation lead to shifts in CL and VB spectra. An increase in downward band bending with increase in surface oxide was observed. The VB analysis revealed that GaN film have N2p-Ga4p, N2p-Ga4s\*, mixed and N2p-Ga4s hybridization states. Surface pits were identified as ideal site for oxide formation due to favourable energetics. The increase in average pit density and pit depth lead to increase in the contribution of oxide. The rms roughness of the surface also increased with surface oxidation.

## Acknowledgement:

The authors are thankful to Director, CSIR-NPL India for his immense support. This work is financially supported by Council of Scientific and Industrial Research, India under the XII<sup>th</sup>-FYP-PSC-0109. One of the co-author (SKTC) would like to thank DST (GoI) and SIMCO Global Tech. & System Ltd. for financial support under Prime Minister doctoral fellowship.

## References:

1. Lin, Y.-J.; Ker, Q.; Ho, C.-Y.; Chang, H.-S.; Chien, F.-T.; Nitrogen-vacancy-related defects and Fermi level pinning in n-GaN Schottky diodes, *J. Appl. Phys.* 2003, 94, 1819-22.
2. Mishra, M.; T.C. Krishna, S.; Aggarwal, N.; Gupta, G.; Surface chemistry and electronic structure of nonpolar and polar GaN films, *Appl. Surf. Sci.* 2015, 345, 440-447.
3. Krukowski, S.; Kempisty, P.; Strk, P.; Fermi level influence on the adsorption at semiconductor surfaces-ab initio simulations, *J. Appl. Phys.* 2013, 114, 063507-17.
4. Xu, X.; Liu, X.; Guo, Y.; Wang, J.; Song, H.; Yang, S.; Wei, H.; Zhu, Q.; Wang, Z.; Influence of band bending and polarization on the valence band offset measured by x-ray photoelectron spectroscopy, *J. Appl. Phys.* 2010, 107, 104510-16.
5. Karrer, U.; Ambacher, O.; Stutzmann, M.; Influence of crystal polarity on the properties of



- Pt/GaN Schottky diodes, *Appl. Phys. Lett.* 2000, 77, 1012-14.
6. Tsai, C.-L.; Fu, Y.-K.; Chen, H.-T.; Chou, C.-H.; Xuan, R.; Investigation of the Ti/Al/Pt/Au and Ti/Au contact material on the N-face surface of oxygen doped GaN, *Phys. Stat. Sol. C* 2014, 11, 957-60.
  7. Oyama, S.; Hashizume, T.; Hasegawa, H.; Mechanism of current leakage through metal/n-GaN interfaces, *Appl. Surf. Sci.* 2002, 190, 322-25.
  8. Hao, Y.; Yang, L.; Ma, X.; Ma, J.; Cao, M.; Pan, C.; Wang, C.; Zhang, J.; High-Performance Microwave Gate-Recessed AlGaIn/GaN/GaN MOS-HEMT With 73% Power-Added Efficiency, *IEEE Elec. Dev. Lett.* 2011, 32, 626-28.
  9. Miao, M.S.; Weber, J.R.; Van de Walle, C.G.; Oxidation and the origin of the two-dimensional electron gas in AlGaIn/GaN heterostructures, *J. Appl. Phys.* 2010, 107, 123713-24.
  10. Elsner, J.; Gutierrez, R.; Hourahine, B.; Jones, R.; Haugk, M.; Frauenheim, Th.; A Theoretical study of O chemisorption on GaN (0001)/(000-1) surfaces. *Sol. Stat. Comm.* 1998, 108, 953-58.
  11. Bermudez, V.M.; Study of oxygen chemisorption on the GaN (0001)(1×1) surface, *J. Appl. Phys.* 1996, 80, 1190-1200
  12. Prabhakaran, K.; Andersson, T.G.; Nozawa, K.; *Appl. Phys. Lett.* 1996, 69, 3212-14.
  13. Liu, Q.Z.; Lau, S.S.; A review of the metal-GaN contact technology, *Sol. Stat. Elec.* 1998, 677-91.
  14. Shalish, I.; Shapira, Y.; Burstein, L.; Salzman, J.; Surface states and surface oxide in GaN layers, *J. Appl. Phys.* 2001, 89, 390-95.
  15. Tajima, M.; Kotani, J.; Hashizume, T.; Effects of Surface Oxidation of AlGaIn on DC Characteristics of AlGaIn/GaN High-Electron-Mobility Transistors, *Jap. J. Appl. Phys.* 2009, 48, 020203-06.
  16. Cao, X.A.; Pearton, S.J.; Dang, G.; Zhang, A.P.; Ren, F.; Van, J.M.; Effects of interfacial oxides on Schottky barrier contacts to n- and p-type GaN, *Appl. Phys. Lett.* 1999, 75, 4130-33.
  17. Gao, F.; Lu, B.; Li, L.; Kaun, S.; Speck, J.S.; Thompson, C.V.; Palacios, T.; Role of oxygen in the OFF-state degradation of AlGaIn/GaN high electron mobility transistors, *Appl. Phys. Lett.* 2011, 99, 223506-09.
  18. Liu, H.-P.; Chen, I.-G.; Tsay, J.-D.; Liu, W.-Y.; Guo, Y.-D.; Hsu, J.-T.; Influence of Growth Temperature on Surface Morphologies of GaN Crystals Grown on Dot-Patterned Substrate by Hydride Vapor Phase Epitaxy, *J. Electroceram.* 2004, 13, 839-46.
  19. Gracia, M.A.S.; Calleja, E.; Monroy, E.; Sanchez, F.J.; Calle, F.; Munoz, E.; Beresford, R.; The effect of the III/V ratio and substrate temperature on the morphology and properties of GaN- and AlN-layers grown by molecular beam epitaxy on Si(1 1 1), *J. Crys. Grow.* 1998, 183, 23-30.
  20. Du, D.; Srolovitz, D.J.; Faceted dislocation surface pits, *Acta Materialia* 2004, 52, 3365-74.
  21. Northup, J.E.; Romano, L.T.; Neugebauer, J.; Surface Energetics, pit formation, and chemical ordering in InGaIn alloys, *App. Phys. Lett.* 1999, 74, 2319-21.
  22. Mishra, M.; Krishna TC, S.; Rastogi, P.; Aggarwal, N.; Chauhan, A.K.S.; Goswami, L.; Gupta, G.; New Approach to Clean GaN Surfaces, *Mater. Focus* 2014, 3, 218-23.
  23. Mishra, M.; Krishna TC, S.; Aggarwal, N.; Vihari, S.; Chauhan, A K S; Gupta, G; A Comparative Photoelectron Spectroscopic Analysis of MBE and MOCVD Grown Epitaxial GaN Films, *Sci. Adv. Mater.* 2015, 7, 546-51.
  24. Thakur, V.; Shivaprasad, S.M.; Electronic structure of GaN nanowall network analysed by XPS, *Appl. Surf. Sci.* 2015, 327, 389-93.
  25. Eisenhardt, A.; Lorenz, P.; Himmerlich, M.; Gutt, R.; Schaefer, J.A.; Krischok, S.; Interaction of Oxygen and Water with Group III-Nitride (InN, GaN) surfaces, *World J. Eng.* 2009, 6, 211.
  26. Foster, C.M.; Collazo, R.; Sitar, Z.; Ivanisevic, A.; Aqueous Stability of Ga- and N-Polar Gallium Nitride, *Langmuir* 2013, 29, 216-220.
  27. Shen, X.; Allen, P.B.; Hybertsen, M.S.; Muckerman, J.T.; Water Adsorption on the GaN (101j0) Nonpolar Surface, *J. Phys. Chem. C Lett.* 2009, 113, 3365-3368.
  28. Chen, Y.; Kuo, J.; Density Functional Study of the First Wetting Layer on the GaN (0001) Surface, *J. Phys. Chem. C* 2013, 117, 8774-8783.
  29. Lambrecht, W.R.L.; Segall, B.; Strite, S.; Martin, G.; Agarwal, A.; Morkoc, H.; Rockett, A.; X-ray Photoelectron Spectroscopy and Theory of the Valence band and Semicore Ga 3d states in GaN, *Phys. Rev. B* 1994, 50, 14155-60.
  30. Lorenz, P.; Haensel, T.; Gutt, R.; Koch, R.J.; Schaefer J.A.; Krischok, S.; Analysis of Polar GaN Surfaces with Photoelectron and High Resolution Electron Energy Loss Spectroscopy, *Phys. Status Solidi B* 2010, 247, 1658-61.
  31. Skuridina, D.; Dinh, D.V.; Lacroix, B.; Ruterana, P.; Hoffmann, M.; Sitar, Z.; Pristovsek, M.; Kneissl, M.; Vogt, P.; Polarity Determination of Polar and Semipolar (1122) InN and GaN layers by Valence Band Photoemission Spectroscopy, *J. Appl. Phys.* 2013, 114, 173503-06.
  32. Veal, T.D.; King, P.D.C.; Jefferson, P.H.; Piper, L.F.J.; McConville, C.F.; Lu, H.; Schaff, W.J.; Anderson, P.A.; Durbin, S.M.; Muto, D.; Naoi, H.; Nanishi, Y.; In adlayers on c-plane InN Surfaces: A Polarity-dependent study by X-ray

- Photoemission Spectroscopy, Phys. Rev. B 2007, 76, 075313-18.
33. Magnuson, M.; Mattesini, M.; Höglund, C.; Birch, J.; Hultman, L.; Electronic structure of GaN and Ga investigated by soft x-ray spectroscopy and first-principles methods, Phys. Rev. B 2010, 81, 085125(1)–085125(8).
34. Hasegawa, H.; Inagaki, T.; Ootomo S.; Hashizume, T.; Mechanisms of Current Collapse and Gate leakage Currents in AlGaIn/GaN Heterostructure field effect Transistors, J. Vac. Sci. Technol. B. 2003, 21, 1844-55.
35. Segav, D.; Van de Walle, C.G.; Origins of Fermi-level pinning on GaN and InN Polar and Nonpolar Surfaces, Europhys. Lett. 2006, 76, 305-11.
36. Tracy, K.M.; Mecouch, W.J.; Davis, R.F.; Nermanich, R.J.; Preparation and Characterization of Atomically Clean, Stoichiometric Surfaces of n- and p-type GaN (0001), J. Appl. Phys. 2003, 94, 3163-72.
37. Hong, S.K.; Yao, T.; Kim, B.J.; Yoon, S.Y.; Kim, T.I.; Origin of hexagonal-shaped etch pits formed in (0001) GaN films, Appl. Phys. Lett. 2000, 77, 82-84
38. Heying, B.; Averbeck R.; Chen, L.F.; Haus, E.; Riechert, H.; Speck, J.S.; Control of GaN surface morphologies using plasma-assisted molecular beam Epitaxy, J. Appl. Phys. 2000, 88, 1855-60.
39. Baik, K.H.; Kim, J.; Characterization of hexagonal defects in gallium nitride on sapphire, J. Ceram. Pro. Res. 2007, 8, 277-80.
40. Paskova, T.; Glodys, E.M.; Monemar, B.; Hydride vapour-phase epitaxy growth and cathodoluminescence characterisation of thick GaN films, J. Crys. Grow. 1999, 203, 1-11.
41. Hawkridge, M.E.; Cherns, D.; Oxygen Segregation to dislocations in GaN, Appl. Phys. Lett. 2005, 87, 221903-05.
42. Butcher, K.S.A.; Timmers, H.; Afifuddin, Chen, P.P.T.; Weijers, T.D.M.; Goldys, E.M.; Tansley, T.L.; Elliman, R.G.; Freitas, J.A.; Crystal size and oxygen segregation for polycrystalline GaN, J. Appl. Phys. 2002, 92, 3397-03.
43. Tarsa, E.J.; Heying, B.; Wu, X.H.; Fini, P.; DenBaars, S.P.; Speck, J.S.; Homoepitaxial growth of GaN under Ga-stable and N-stable conditions by plasma-assisted molecular beam epitaxy, J. Appl. Phys. 1997, 82, 5472-79.
44. Zywiets, T.; Neugebauer, J.; Scheffler, M.; adatom diffusion at GaN (0001) and (000 $\bar{1}$ ) surfaces, Appl. Phys. Lett. 1998, 73, 487-90.

# Pits Assisted Oxygen Chemisorption on GaN Surfaces

Monu Mishra<sup>§†</sup>, Shibin Krishna TC<sup>§†</sup>, Neha Aggarwal<sup>§†</sup>, Mandeep Kaur<sup>§</sup>, Sandeep Singh<sup>#</sup> and Govind Gupta<sup>§†\*</sup>

<sup>†</sup> Surface Physics and Nanostructure Heteroepitaxy, Physics of Energy Harvesting Division, CSIR-National Physical Laboratory, Dr. K.S. Krishnan Marg, New Delhi-110012, India.

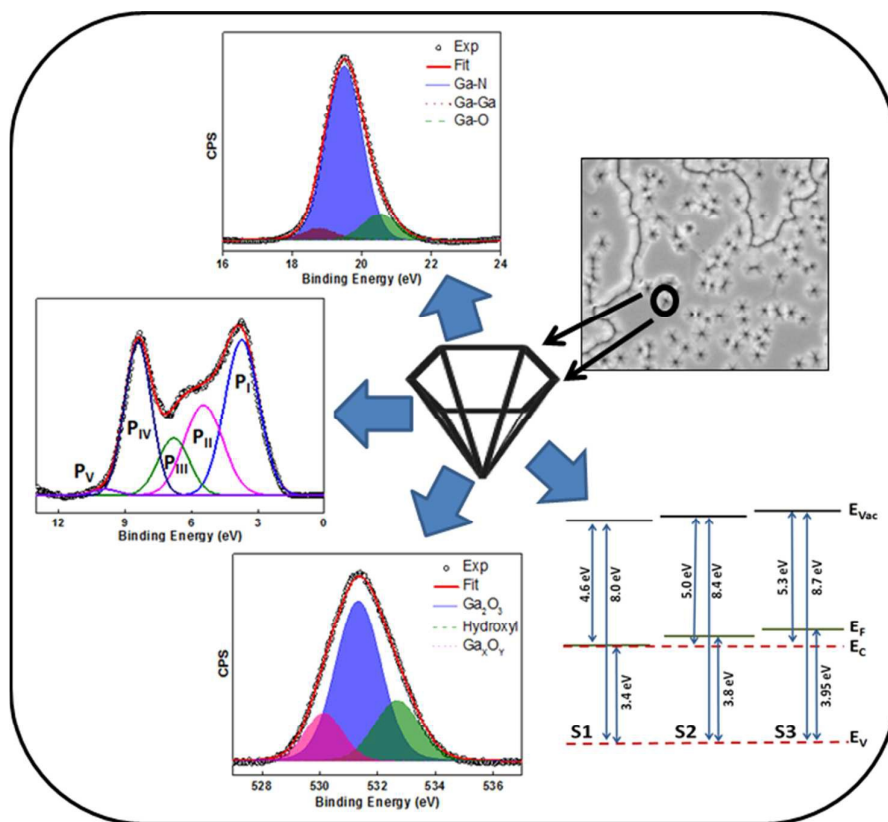
<sup>§</sup> Quantum Phenomena and Applications, CSIR-National Physical Laboratory, Dr. K.S. Krishnan Road, New Delhi-110012, India.

<sup>#</sup> Sophisticated and Analytical Instrumentation, CSIR-National Physical Laboratory, Dr. K.S. Krishnan Road, New Delhi-110012, India.

<sup>§</sup> Academy of Scientific and Innovative Research (AcSIR), CSIR-NPL Campus, Dr. K.S. Krishnan Road, New Delhi-110012, India.

\*Corresponding Author: [govind@nplindia.org](mailto:govind@nplindia.org), Tel: +91-11-45608403, Fax: +91-11-4560-9310

## Graphical Abstract



We correlate the oxygen chemisorption on GaN films with pits structure. The surface pits acted as a favourable site for oxygen chemisorption due to their favourable energetics, which resulted in significant changes in electronic properties and energy band structure.